Geodetic effects of the ocean response to atmospheric forcing in an ocean general circulation model

O. de Viron
Royal Observatory of Belgium, Brussels, Belgium

J.-P. Boy[1]
NASA Goddard Space Flight Center, Greenbelt, Maryland, USA

H. Goosse
Institut d'Astronomie et de Géophysique Georges Lemaitre, Université catholique de Louvain, Louvain-La-Neuve, Belgium

Received 9 October 2003; revised 29 January 2004; accepted 4 February 2004; published 26 March 2004.

[1] We have adapted the Coupled Large-scale Ice-Ocean (CLIO) model in order to include atmospheric pressure forcing in addition to the classical atmospheric forcing (heat and freshwater fluxes and wind stress). We have compared the modeled bottom pressure to in situ bottom pressure measurements and also to another ocean model. We have computed the induced effects on Earth orientation parameters (polar motion and nutations) and also on Earth time-variable gravity field. We show that the response of the ocean to atmospheric pressure forcing has geodetic consequences well above the precision level and that the response of CLIO seems reasonable with respect to the few data sets we can compare with. We also show that the results obtained from the model improve the modeling of polar motion. *INDEX TERMS:* 1214 Geodesy and Gravity: Geopotential theory and determination; 1210 Geodesy and Gravity: Diurnal and subdiurnal rotational variations; 1223 Geodesy and Gravity: Ocean/Earth/atmosphere interactions (3339); 1239 Geodesy and Gravity: Rotational variations; *KEYWORDS:* Earth-ocean-atmosphere interaction, Earth rotation, gravity

Citation: de Viron, O., J.-P. Boy, and H. Goosse (2004), Geodetic effects of the ocean response to atmospheric forcing in an ocean general circulation model, *J. Geophys. Res.*, *109*, B03411, doi:10.1029/2003JB002837.

1. Introduction

[2] The most important variables studied in geodesy, such as those related to the shape of the Earth, its gravitational potential and its rotational motion, are now monitored with an incredibly high precision. For example, three-dimensional (3-D) surface displacements can nowadays be monitored by Global Positioning System (GPS) or very long baseline interferometry (VLBI) at a subcentimeter level and superconducting gravimeters record surface gravity changes at the nanoGal (10^{-11} m/s^2) level. The Earth orientation in space and its variations are now measured at the millimeter level and Earth's gravity field variations are resolved by the Gravity Recovery and Climate Experiment (GRACE) mission [*Dickey et al.*, 1997] with an accuracy of 1 mm in terms of geoid height over wavelengths larger than a few hundred of kilometers.

[3] The geodetic quantity variations are also modeled, and the confrontation with the observations helps us to improve our knowledge of the Earth shape, potential, and orientation and to better understand the Earth as a complex system [see, e.g., *Munk and McDonald*, 1960]. The geodetic observations see the Earth as a whole, and only the total effects, coming from the different parts of the Earth system, are obtained. It is one of the biggest challenge for this area of geodesy to separate the effects from the different sources. For instance, the variations of the Earth orientation in space are due to a combination of effects coming from the atmosphere, the ocean, the hydrology, the Earth's mantle, the Earth's core, and even the other planets [see, e.g., *Dehant and de Viron*, 2002]. Consequently, the interpretation in terms of geophysics is very difficult.

[4] Because of constant improvements of observation techniques, previously negligible phenomena can now be observed. On the one hand, geodesy can be used to monitor mass redistribution within the surface fluid layers [see *Chao*, 2003]; on the other hand, these effects need to be carefully removed from the observation data for studying the Earth's deep interior. The classical approach for modeling and correcting these loading effects induced by surface fluid layers is to use global circulation models (GCM) outputs; atmospheric effects are modeled using meteorological analysis models. Most of these models have been

[1]Now at Ecole et Observatoire des Sciences de la Terre, Institut de Physique du Globe, Université Strasbourg, Strasboug, France.

0148-0227/04/2003JB002837$09.00

developed for other purposes, such as weather forecasts, and therefore do not always meet the needs of geodesy. For example, because of the high sampling rate of most geodetic techniques or because of potential aliasing problems of space gravity missions, there is a crucial need of modeling high-frequency (subdiurnal to hourly) signals induced by atmospheric or oceanic circulations. [*Yseboodt et al.*, 2002] have shown that atmospheric models differ significantly from each other at the retrograde diurnal frequency, as seen in the atmospheric effect on nutation.

[5] We here focus on the signals induced by nontidal ocean circulation, and more particularly induced by the ocean response to pressure forcing. Most of the ocean global circulation models (OGCM) implicitly assume the inverted barometer (IB) approximation for describing the ocean response to atmospheric pressure forcing; that is, atmospheric pressure variations are compensated by static sea height variations. This assumption has been shown to be valid for periods typically larger than 2–3 weeks [*Wunsch and Stammer*, 1997], but for shorter periods the real response of the oceans significantly differs from the IB model [*Tierney et al.*, 2000]. Until now, the only models that include a direct forcing by atmospheric pressure are 2-D barotropic models [e.g., *Ponte*, 1993; *Ponte and Ali*, 2002]. Barotropic models assume only a 2-D dynamics of the ocean, with all the variable being constant vertically, whereas baroclinic models represent the full 3-D dynamics of the ocean. As the high-frequency dynamics of the ocean is mostly barotropic, the 2-D models succeed reasonably in modeling the short-period behavior of the ocean but cannot be used when the period is long enough so that the thermodynamics plays an important role. In particular, those models are able to explain most of the high-frequency (period shorter than 5 days) polar motion as shown by *Ponte and Ali* [2002], but because of the 3-D structure of the ocean that is neglected in those models, they fail to predict geodetic effects of the oceans at longer timescales. Additionally, the low-frequency baroclinic dynamics of the ocean modulates the high-frequency response to the atmospheric forcing.

[6] On the other hand, several more complex (baroclinic) OGCM has been successful in predicting long-term length-of-day (LOD) variations [*Marcus et al.*, 1998], slow polar motion (PM) [*Ponte et al.*, 1998; *Gross*, 2000], and long-term gravity changes [*Dickey et al.*, 2002]. However, because all these models are only forced by heat fluxes, atmospheric winds, and possibly freshwater fluxes (possibly sea-ice interactions, etc.), and not by atmospheric pressure, they cannot be used for modeling high-frequency ocean circulation and their induced geodetic effects.

[7] In order to reproduce both the high- and low-frequency variations, the simulations must be performed with a 3-D model, including both barotropic and baroclinic dynamics, driven by pressure in addition to the classical forcing. Here we propose analyzing the results of such simulations. A description of the model used (called CLIO for Coupled Large-scale Ice-Ocean) is given in section 2. We discuss the ocean response to pressure forcing modeled by CLIO, and we compare our results with previous studies in section 3. The effects of this nontidal ocean model on Earth's rotation (polar motion and nutations) and on Earth's time-variable gravity field are shown in sections 4 and 5, respectively. Discussions and concluding remarks are given in section 6.

2. Description of the Model and Simulations Used in This Study

[8] The CLIO model [*Goosse et al.*, 2000] used here is made up of a three-dimensional global ocean general circulation model (OGCM) coupled to a comprehensive thermodynamic-dynamic sea ice model. The OGCM is a primitive equation, free surface model that rests on the usual set of assumptions, i.e., the hydrostatic equilibrium and the Boussinesq approximation [*Deleersnijder and Campin*, 1995]; *Campin and Goosse*, 1999]. It contains a formulation of the subgrid-scale vertical mixing derived from the *Mellor and Yamada* [1982] level 2.5 turbulence closure scheme [*Goosse et al.*, 1999], a parameterization of density-driven downslope flows [*Campin and Goosse*, 1999], the *Gent and McWilliams* [1990] parameterization of the tracer transport due to mesoscale eddies, and a physically based representation of the upper boundary condition for the salinity balance [*Tartinville et al.*, 2001]. In the sea ice model [*Fichefet and Morales Maqueda*, 1997], sensible heat storage and vertical heat conduction within snow and ice are determined by a three-layer model (one layer for snow and two layers for ice). The model also allows for the presence of open water (i.e., leads) within the ice pack. For the momentum balance, sea ice is considered as a two-dimensional continuum in dynamical interaction with atmosphere and ocean. The viscous-plastic constitutive law proposed by *Hibler* [1979] is used for calculating the internal ice force. The coupled model has a horizontal resolution of 1.5 degree, and there are 30 unequally spaced vertical levels in the ocean. The bathymetry is a discretized version of the real world ocean bottom topography. For the purpose of the present analysis, the effect of variations of atmospheric pressure at the ocean surface has been included as an additional forcing term in the ocean momentum equation solved by the model. Daily surface air temperatures and winds from the National Centers for Environmental Prediction National Center for Atmospheric Research (NCEP-NCAR) reanalysis project for the period 1991–2002 [*Kalnay et al.*, 1996] are utilized to drive the model. The other atmospheric input fields consist of climatological monthly surface relative humidities, cloud fractions, precipitations, and rivers runoff prescribed according to various monthly climatology. Furthermore, a relaxation toward observed annual mean salinities [*Levitus*, 1982] is applied in the 10-m-thick surface grid box with a time constant of 2 months. For more details about the forcing, see *Goosse et al.* [2000] or *Fichefet et al.* [2003]. As shown in previous studies [e.g., *Goosse et al.*, 1999; *Fichefet et al.*, 2003], the model simulated reasonably well the observed evolution of the ocean and the sea ice.

[9] For the present study, two runs are analyzed. They have exactly the same forcing and characteristics, except for the pressure forcing, every 6 hours, which is only used in one of the runs (non-IB and IB). The mass conservation in

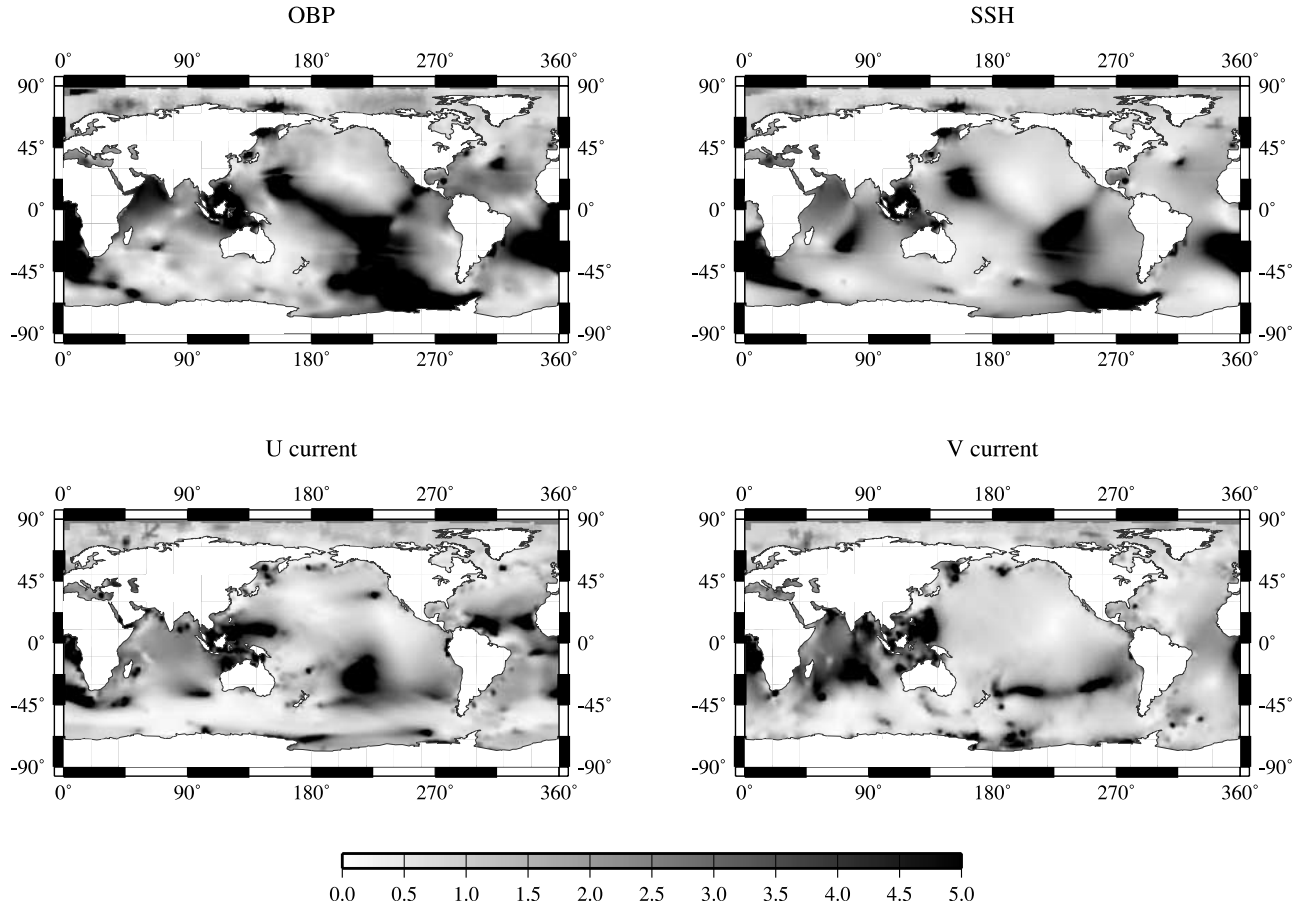

Figure 1. Ratio between the two CLIO runs (IB and pressure forcing) and the IB run at S_1 frequency.

the model is imposed for both runs by adding a uniform water layer over the whole ocean.

3. Ocean Response to Atmospheric Pressure Forcing

[10] The ocean response to pressure forcing is commonly modeled as an IB process for periods exceeding 2–3 weeks. The ocean is therefore supposed to react stactically to pressure change $p_a(\theta, \lambda, t)$ by sea height variations $\eta(\theta, \lambda, t)$ [*Wunsch and Stammer*, 1997]:

$$\eta(\theta, \lambda, t) = -\frac{p_a(\theta, \lambda, t) - \bar{p}_a(t)}{\rho_w g_0}, \qquad (1)$$

where ρ_w and g_0 are the mean ocean density and the mean Earth gravity field; $\bar{p}_a(t)$ is the instantaneous mean atmospheric pressure over the oceans (this term is introduced in order to conserve the total ocean mass). It is further assumed that the ocean has enough time to come back to equilibrium so that there is no current associated to the IB ocean reaction. The IB hypothesis becomes therefore invalid when the ocean has not enough time to react, i.e., for periods shorter than a couple of weeks [*Ponte and Gaspar*, 1999]. The IB hypothesis only considers the response of the ocean to pressure forcing and does not include any ocean reaction to freshwater flux, energy transfer, and friction drag. For this reason, it can (and should) be used jointly with oceanic models that only consider those last forcing, as the nonlinearity effects can be neglected.

[11] We compute the ratio between the differences between the two CLIO runs and the IB run for the ocean bottom pressure (OBP), the sea surface height (SSH), and the zonal (U) and the meridional (V) currents. Figure 1 shows this ratio for a composite cycle at the S_1 (1 day) frequency.

[12] The ocean response to atmospheric pressure forcing significantly differs from the IB assumption, especially at low latitudes as shown also in T/P data [*Fu and Pihos*, 1994; *Ponte and Gaspar*, 1999]. The discrepancies are particularly high in the Indian Ocean.

[13] As expected, when the period increases, the differences between the two CLIO runs, i.e., the departure from the IB assumption, decreases. In Figures 2 and 3 we plot the differences between the two CLIO runs as Figure 1 but at the 10- and 60-day periods.

[14] We can notice that the differences in term of currents (U and V) are very small (below 5%), except in the Arctic Ocean at the 10-day period. The differences in bottom pressure and sea surface height changes are typically 2–3 times larger, and large values also appear in the Arctic Ocean. However, the response of the ocean only slightly differs from the IB hypothesis, except in shallow water regions such as, for example, Indonesia, and in the Atlantic.

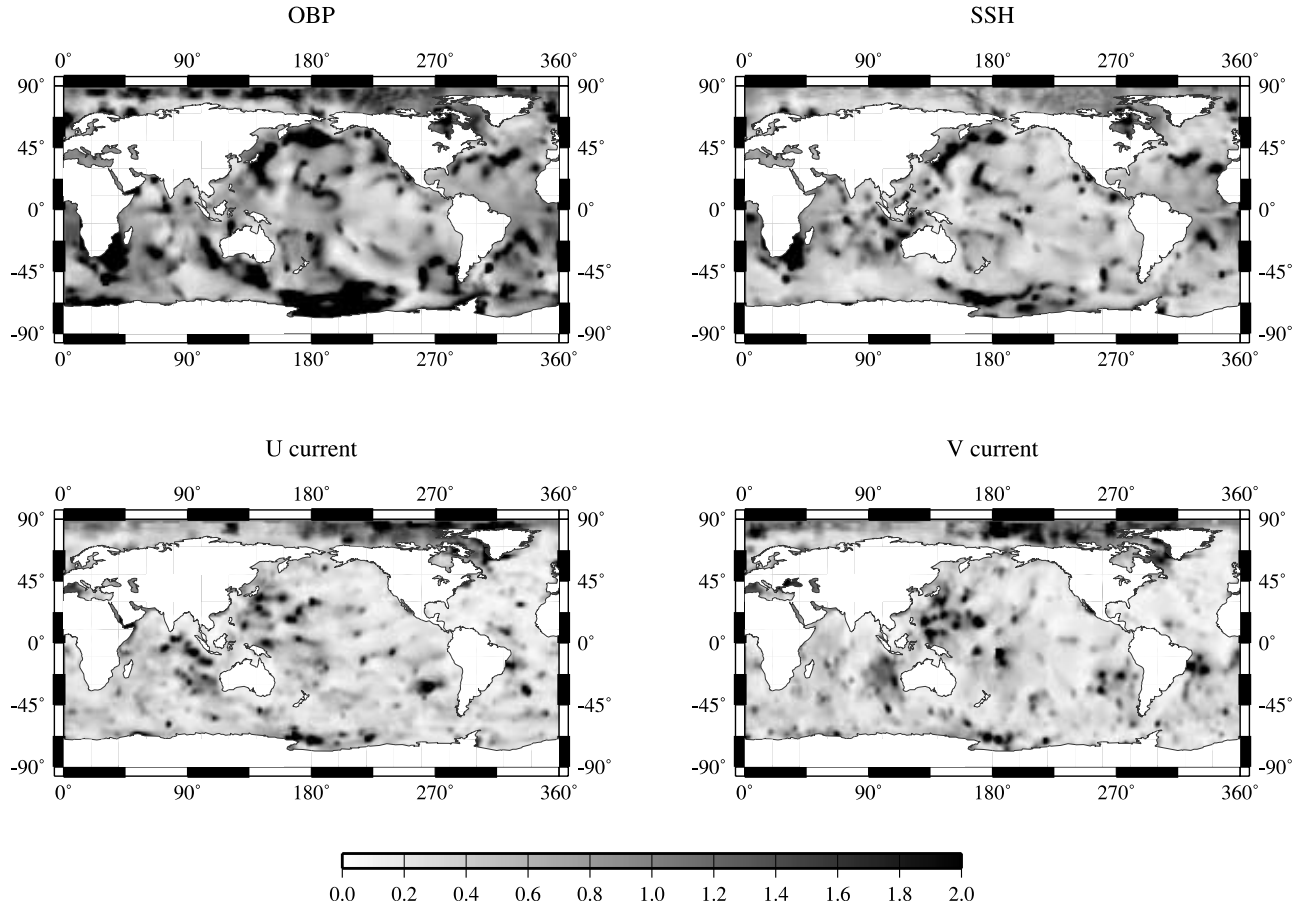

Figure 2. Same as Figure 1 but at 10-day period. Note the change of color scale.

[15] In Figure 4 we show the comparison of the sea bottom pressure changes modeled by CLIO with in situ measurements from the GLOUP (Global Undersea Pressure) data set at five different locations: Amsterdam (Figure 4a), Crozet (Figure 4b) and Kerguelen (Figure 4c) islands in the Indian Ocean, Marfrio in the Atlantic Ocean (Figure 4d), and in the Drake Passage (Figure 4e). Diurnal (S_1) and semidiurnal (S_2) periodic signals have been removed in all time series.

[16] We can notice that there is usually (Figures 4a, 4b, and 4e) a better correlation between OBP observations with the no-IB CLIO model for periods larger than a couple of days. For Kerguelen islands (Figure 4c), the better correlation only appears for periods between 2 and 1 days; The correlation is worst for larger periods. For Marfrio (Figure 4d), there is a better correlation for the IB run.

[17] For higher frequencies, there are no significant differences between the two CLIO runs, at least in term of squared coherence. However, if we plot the time series (see Figure 5), we can notice that the non-IB CLIO model seems to overestimate the ocean response by typically a factor 2 at high frequency. We do not have, at this time, any explanations, but this ocean model was not built to work at very high frequencies, and it is to be expected that it will need some additional adaptation to adequately represent the dynamics at such frequencies. Additionally, it is not unlikely that the atmospheric forcing at that timescale is not correct. Similar problems at high frequency (<2 days) were already documented by *Hirose et al.* [2001].

4. Effect on Polar Motion and Nutation

4.1. Polar Motion

[18] The fluid effect on Earth rotation is computed from the angular momentum conservation of the atmosphere-ocean-solid earth system [see, e.g., *de Viron et al.*, 2002]. The atmospheric angular momentum (AAM) series have been obtained from the International Earth Rotation Service (IERS) Special Bureau for the Atmosphere. As CLIO has been forced by the output of the NCEP reanalysis model [*Kalnay et al.*, 1996], we have to use the AAM from that model, for reasons of consistency. From the CLIO ocean bottom pressure (OBP) and currents, we have computed the ocean angular momentum (OAM). Note that the CLIO OBP only includes the water pressure and not the air pressure. Consequently, the atmospheric pressure has to be added in the mass term, for both runs, if we want to get the mass term of the whole fluid column. The OAM series obtained from the nonpressure forced run have been compared to the ones from *Ponte et al.* [1998], available on the IERS Special Bureau for the Ocean, and are usually reasonably similar, as shown in Figure 6. We add the total AAM (non-IB) to the OAM from the simulation forced by the atmosphere including the pressure. We add the IB-AAM (i.e., the normal wind

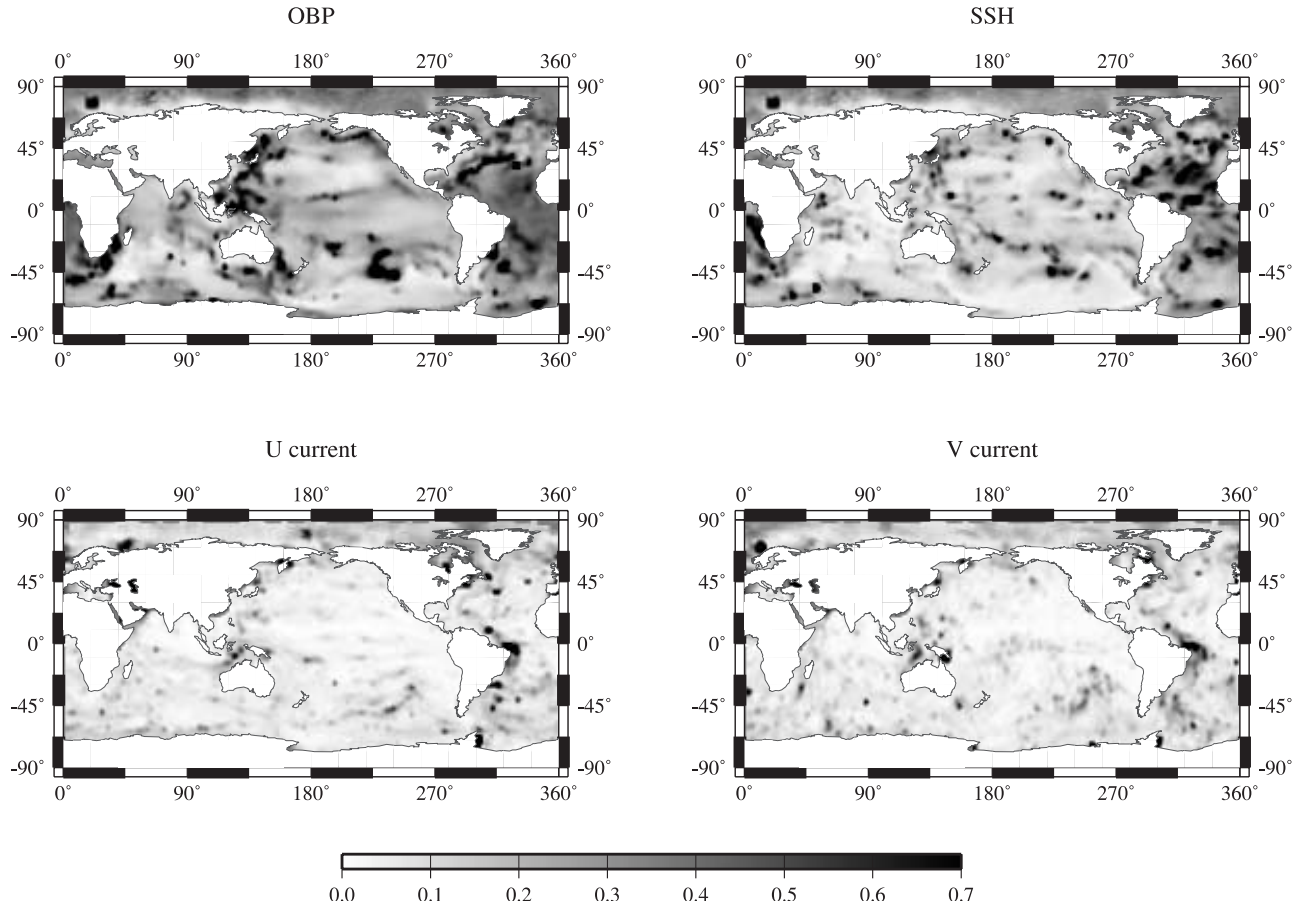

Figure 3. Same as Figure 1 but at 60-day period. Note the change of color scale.

term and the pressure term corrected with the IB assumption) to the OAM from the simulation forced by the atmosphere but not by the pressure.

[19] Though it is commonly accepted that at low frequency, the ocean mostly reacts as an inverted barometer, we have evaluated the effect on polar motion of the non-IB response of our model. In Figure 7 we show the amplitude of the polar motion associated with the difference between the IB and non-IB CLIO results (including the associated atmospheric effect) for a period of between 10 days and 10 years. It can be observed that the effect is above the milliarcsecond (mas) level at interannual timescale, while the observation precision is about 0.2 mas. Because of the resonance at the Chandler wobble, there is also a large difference at that period.

[20] Consequently, the effect of the non-IB ocean response on the polar motion is well above the precision level, even at periods at which the ocean response is generally believed to be adequately represented by the IB hypothesis. As we know that it is important, we need to determine to which extent the pressure forcing improve the polar motion modeling, by comparing its prediction to the geodetic observations.

[21] As shown, for instance, by *Munk and McDonald* [1960], the polar motion (PM) signal is dominated by the beating of two large low-frequency oscillations, an annual wobble, due to the periodicity of the forcing and a resonance at the Chandler wobble. To allow a better comparison with the forcing and, in particular, to avoid instability close to the Chandler wobble frequency, we compared the excitation of PM (by the atmosphere and the ocean) to the excitation deduced from observed PM through the so-called excitation functions, as defined, for instance, by *Barnes et al.* [1983]. In order to test the quality of the CLIO OAM series, both with the IB approximation and with the full atmospheric forcing over the ocean, we have computed the frequency-dependent correlation between the geodetic excitation function and the atmospheric excitation function. As obtained by *Ponte et al.* [1998], the coherence is improved by accounting for the ocean effect. In Figure 8 we show this correlation for the two equatorial components for the period between 10 and 400 days.

[22] It is commonly accepted [see, e.g., *von Mises*, 1964] that the correlation has to be tested using Student's t test, with N-2 degrees of freedom, N being the number of independent data points. This test allows us to determine the minimum correlation coefficient necessary to reject the probability that the correlation observed is only coincidental with only x% of random signals succeeding the test. In our case, it is difficult to assess the number of degrees of freedom, as it depends on the frequency, but 12 can be used, very conservatively, at least for the highest frequencies. In that case, the correlation is significant at the 95% level if the correlation is 0.53. It can be observed that the correlation is better for Y than for X, which is not a big surprise, as there is more continent effect on the X direction,

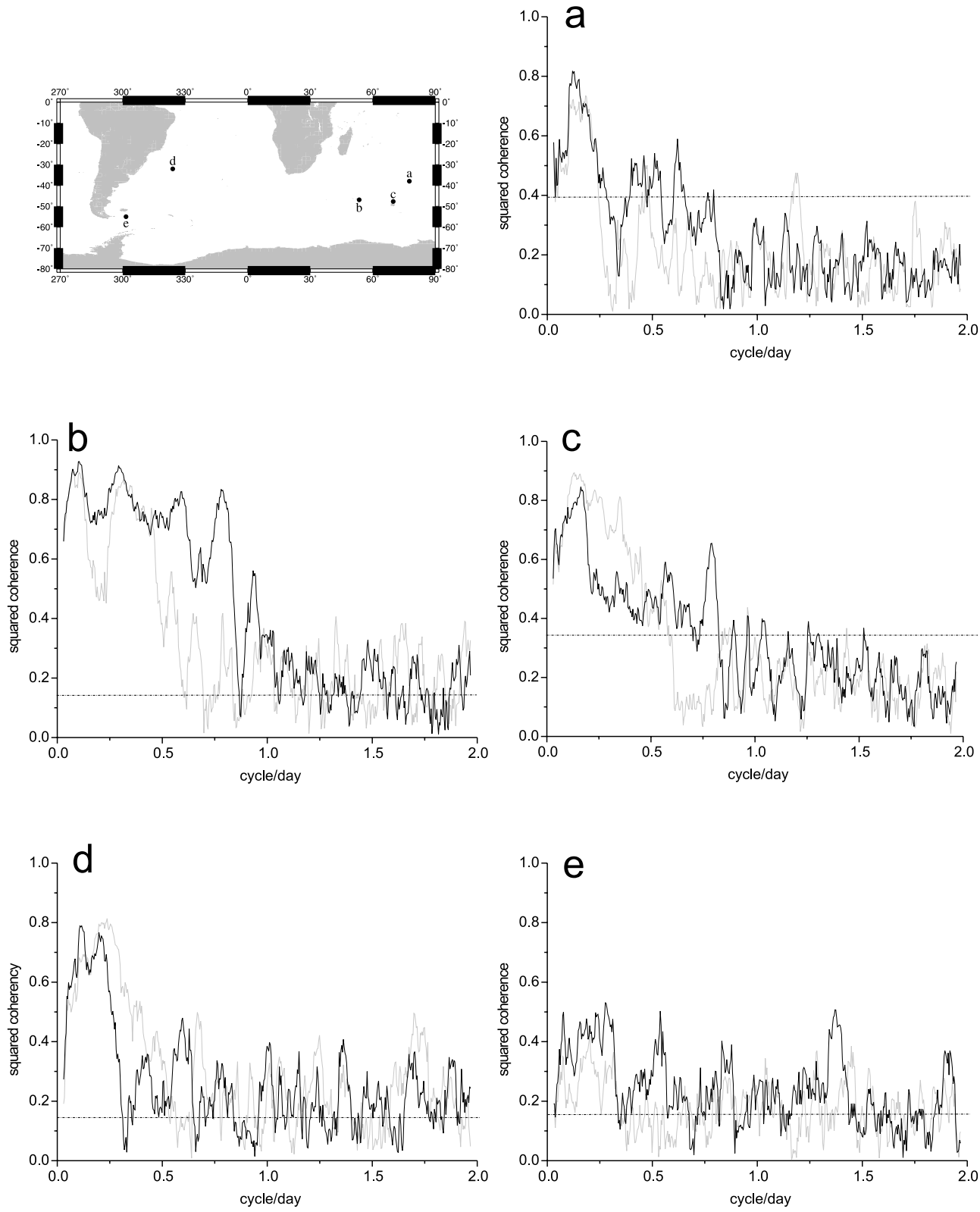

Figure 4. Squared coherency between bottom pressure measurements and bottom pressure modeled by CLIO at five different locations: (a) Amsterdam, (b) Crozet and (c) Kerguelen islands in the Indian Ocean, (d) Marfrio in the Atlantic Ocean, and (e) in the Drake Passage. Gray curve is the IB model, and black curve is the non-IB run. The dot-dashed line shows the 95% confidence.

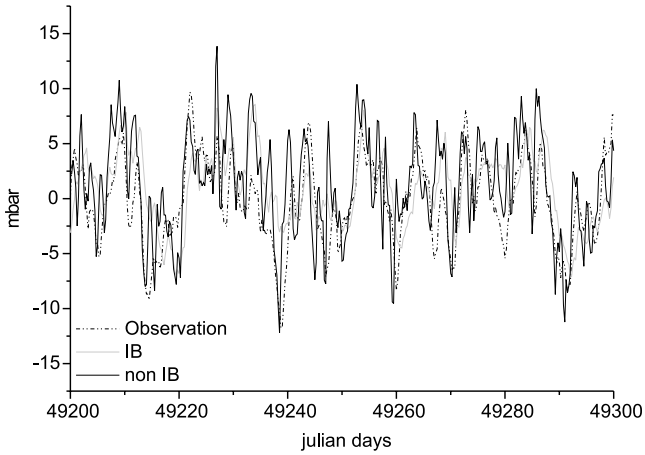

Figure 5. Time series of observed bottom pressure changes and bottom pressure modeled by the two CLIO runs at Crozet (Figure 4b).

which implies a larger role of hydrology. The big drop in correlation at low frequency in the *X* component is associated with an unsuccessful modeling of the annual cycle. At higher frequency, the pressure forced series is slightly better, which is reassuring. Globally, we have found a correlation of 36% (41% with the IB approximation) for the *X* component and 77% (73% with the IB approximation) for the *Y* component. The 95% significance level is at 30% for the total series. It seems that the pressures forcing improve the evaluation of ocean effects on polar motion for *Y*, and the low correlation of the *X* component make the results inconclusive for this component, as part of the forcing (probably the hydrology) is obviously missing.

4.2. Nutation

[23] As shown in section 3, CLIO seems to react a bit too strongly at short periods (shorter than 5 days or so). Nutation results are thus to be taken with caution. Nevertheless, we find it interesting to evaluate what is the order of magnitude to be expected from the effect of the ocean response to atmospheric forcing on the nutation. This effect is only partly taken into account in the nutation model MHB2000 [*Mathews et al.*, 2002], which includes the ocean tidal effect and a constant seasonal term, at the annual prograde nutation frequency (S_1). Actually, the effect of the nontidal dynamics of the ocean at the tidal frequency is also included partly, as most of the up-to-date ocean tide models include assimilation from the TOPEX/Poseidon data, which

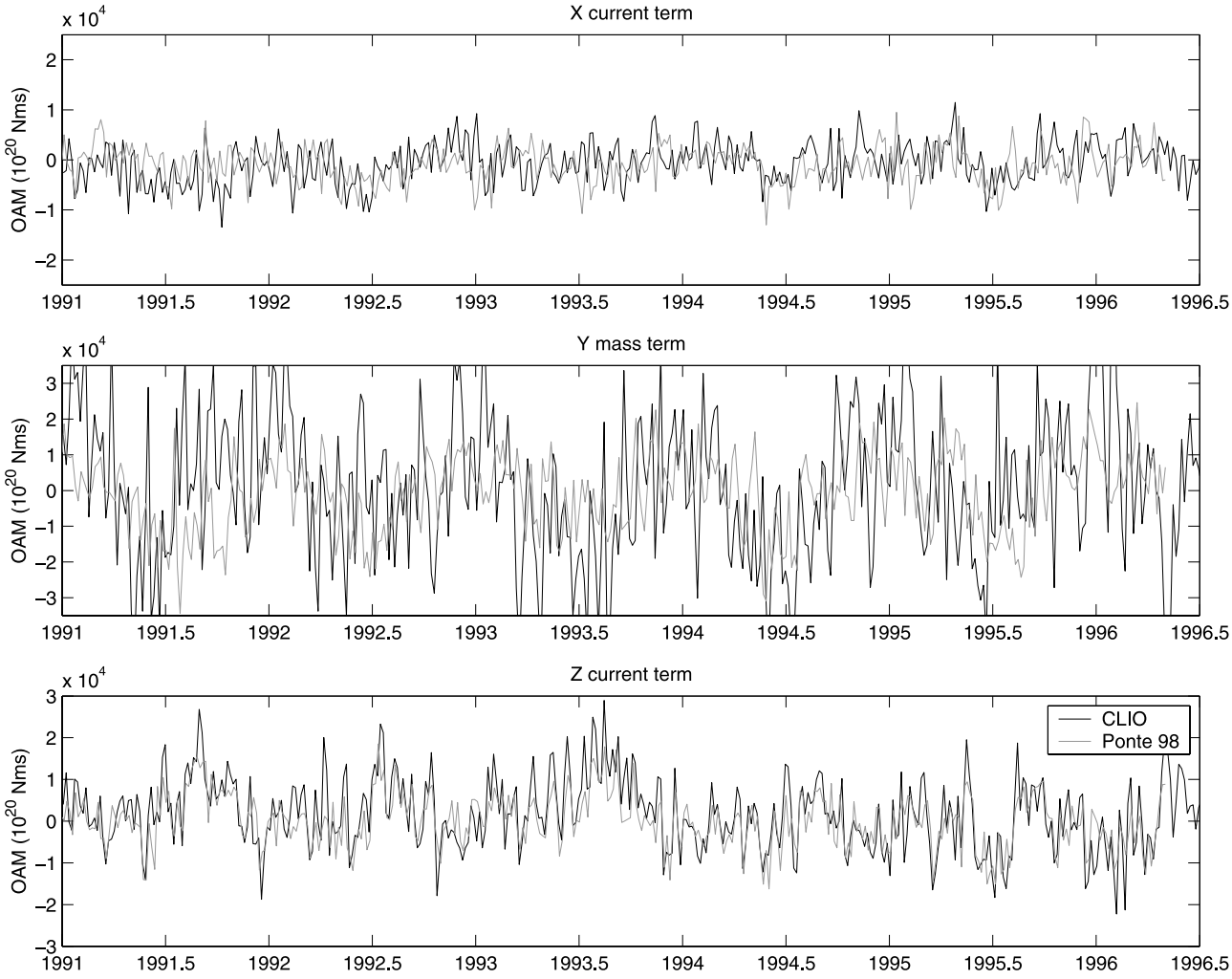

Figure 6. Comparison between some of the OAM series from the *Ponte et al.* [1998] and CLIO models.

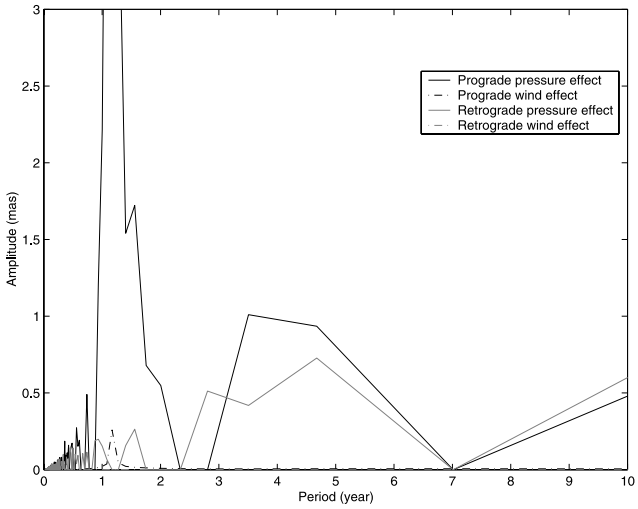

Figure 7. Amplitude of the polar motion in response to the non-IB dynamics of the ocean.

are as sensitive to nontidal ocean effect as to tidal effect. Similarly, the nontidal ocean effect at the S_1 frequency is already partly included in the nutation model, as the amplitude of the seasonal term at that frequency is fitted on the observation.

[24] In Table 1 we show the atmospheric and oceanic effect of the nutation deduced from our computation. The atmospheric effect is computed from the NCEP reanalysis data, as done by *Bizouard et al.* [1998], though the results we have are somewhat different. Those differences are due to the period analyzed, as the results are the same, if the period used is the same as by *Bizouard et al.* [1998]. We limit ourselves to three nutation waves: the semiannual prograde nutation (P_1), the annual prograde nutation (S_1), and the annual retrograde nutation (ψ_1). We did not keep any wave of which the oceanic effect was less than 10 microarc seconds (μas). Additionally, we rejected periods of -420 and -438 days, as they are so close to the free core nutation (FCN) resonance that the noise level would be amplified to reach the detection level. For each period, we show the results obtained with the IB hypothesis and with the full dynamic response of the ocean. Of course, the values of the MHB2000 residuals are the same in both case.

[25] The interpretation of Table 1 is to be done carefully, as MHB2000 is a observation-optimized model. Several parameters of the model (such as the inner core boundary magnetic field, the core-mantle boundary magnetic field) are fitted so that the residuals between MHB2000 and the observation are as small as possible. As the nontidal ocean is not directly included in the model, part of its effect might have been absorbed in another parameter. This is particularly true for P_1 and ψ_1, as a "fluid" effect is estimated for the S_1 frequency: note that the S_1 non-IB estimation of the atmospheric-oceanic effect fit very well the MHB2000 estimation. *Dehant et al.* [2003] have shown that correcting for an atmospheric effect could change slightly the MHB2000 values of the FCN period (by about a day by 10 μas) and quality factor due to change in the amplitudes of the annual retrograde nutation, and the free inner core nutation period (by some tens of days) and quality factor due to change of the semiannual prograde nutation. For the reason explained above, it is difficult to assess if the values for the other waves are reasonable. Nevertheless, no atmospheric effect is included in the MHB2000 model; as the

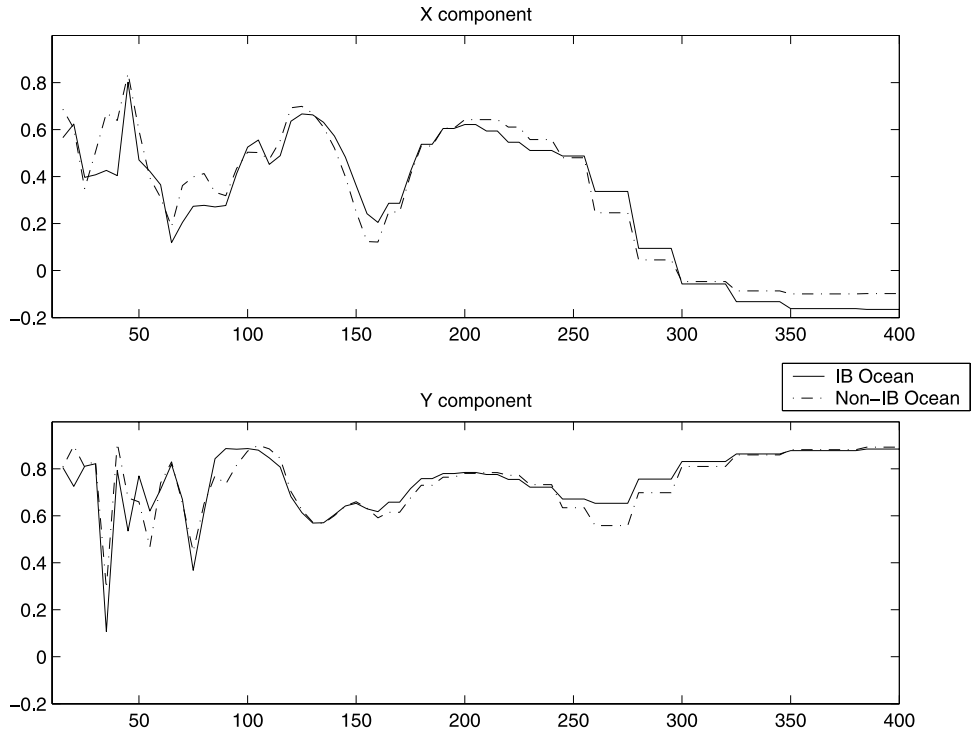

Figure 8. Correlation between the geodetic and ocean-atmosphere polar motion excitation functions, as a function of the period (days); by convention, X is the direction of the Greenwich meridian.

Table 1. Effect of the Atmosphere and Ocean on the Nutation for the Three Nutation Periods With an Ocean Effect Larger Than 10 μas[a]

	Atmosphere		Ocean		Residuals		Total	
	IP	OP	IP	OP	IP	OP	IP	OP
P_1 (IB)	0	−45	−11	−4	−11	−50	0	3
P_1 (non-IB)	−17	−37	0	−5	−17	−42	0	3
S_1 (IB)	17	25	2	89	19	119	−10[b]	108
S_1 (non-IB)	−21	38	8	57	−13	95	−10	108
ψ_1 (IB)	38	6	−54	105	−16	111	8	8
ψ_1 (non-IB)	75	−68	−36	45	39	−23	8	8

[a]The residuals between the MHB2000 nutation model and the VLBI nutation observation are given for comparison. In units of μas.

[b]Note that the MHB2000 model has fitted estimations of the seasonal cycle effect from atmosphere and ocean at the S_1 frequency (in phase and out of phase), with the nutation residuals being zero at that frequency. Consequently, those values are our residuals.

ocean effect is at the same order of magnitude, it does not seem unrealistic.

5. Effect on Gravity Field Changes

[26] The retrieval of hydrologic and oceanic signals in monthly time-variable Earth's gravity field recovered by GRACE requires a precise knowledge of other contributions such as atmospheric loading effects [*Wahr et al.*, 1998]. The precise monthly determination of Stokes coefficients needs especially an efficient estimation of high-frequency perturbations on the satellite orbit determination which will otherwise be aliased in GRACE solutions. Major sources of high-frequency variations of the Earth gravity field are induced by the atmosphere and the oceans. Atmospheric loading effects should be modeled by considering the three-dimensional structure of the atmosphere [see, e.g., *Swenson and Wahr*, 2002]. However, high-frequency nontidal oceanic contributions have also to be modeled with the same accuracy as atmospheric loading effects, which is not the case now.

[27] We therefore computed the Earth's gravity field variations induced by the two runs of the CLIO model. The geoid height variations, of degree n and order m, induced by ocean bottom pressure changes $\Delta p(\theta, \lambda)$ are equal to [*Wahr et al.*, 1998]

$$C_n^m + iS_n^m = \frac{3}{4\pi g_0 \rho_0 (2n+1)} \int\int \Delta p(\theta,\lambda) P_n^m(\cos\theta) e^{im\lambda} \cdot \sin\theta \, d\theta d\lambda, \quad (2)$$

where g_0 and ρ_0 are the mean Earth gravity and density. P_n^m are the (4π) fully normalized Legendre polynomials [*Heiskanen and Moritz*, 1967].

[28] Figure 9 shows the spectrum of the geoid height differences between these two runs, i.e., the differences between the IB and the modeled response to pressure forcing, for different periods, and also the expected accuracy of GRACE (S. Bettadpur, personal communication, 2002). Because the aliasing effects are not easy to model [see, e.g., *Ray et al.*, 2003], we choose to compare the differences between the two CLIO runs to the expected GRACE resolution. Therefore we just show the order of magnitude of the possible aliasing problems due to the mismodeling of the ocean response to pressure forcing. In

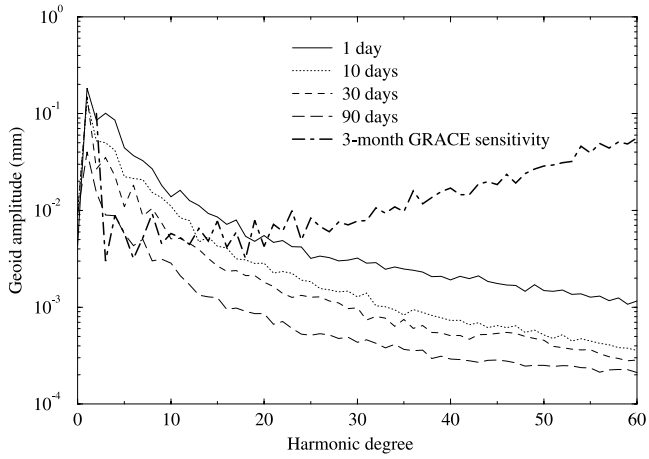

Figure 9. Spectrum of geoid height variations induced by the departure from the IB assumption as modeled by CLIO.

Figure 10 we also plot the differences between the two CLIO runs (i.e., the departure from IB hypothesis) and the total ocean signal (CLIO forced by winds, heat fluxes, and pressure) at 5- and 60-day periods. When the period increases, the discrepancies between the two CLIO runs decrease as opposed to the total ocean contribution which is increasing, at least up to the annual cycle. The pressure forcing is therefore one of the major sources of OBP and SSH variabilities. As pointed out by *Fu and Pihos* [1994], the wind forcing plays also a key role at low latitudes for modeling the oceanic circulation. For periods longer than typically 1 month, the global ocean circulation is mainly forced by winds and heat fluxes.

[29] Figure 11 shows the spatial pattern of the geoid height differences for the periods of 1, 10, 30, and 90 days. We can retrieve in Figure 11 the same general pattern as in the spatial OBP differences between the two CLIO runs (Figures 1–3). We want to point out high discrepancies in Indian Ocean at high frequency, also affecting the Arabian Peninsula. Because of its low hydrological contribution over hundreds of kilometers, this area was proposed to calibrate/validate GRACE products [*Velicogna et al.*, 2001].

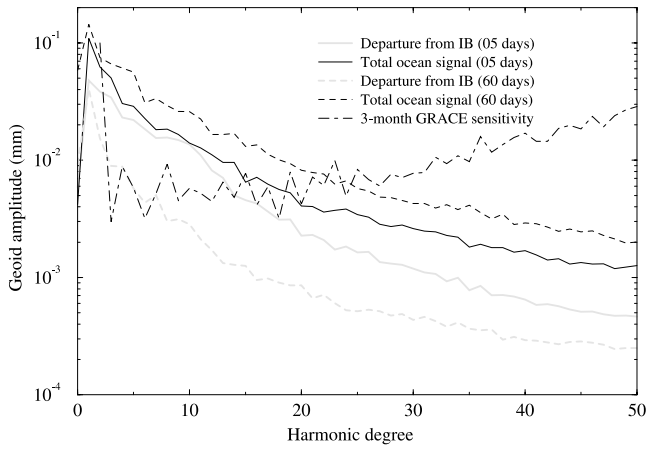

Figure 10. Spectrum of geoid height variations induced by the total ocean contribution (run forced by atmospheric pressure, surface winds and heat fluxes) and differences with the IB run at 5- and 60-day periods.

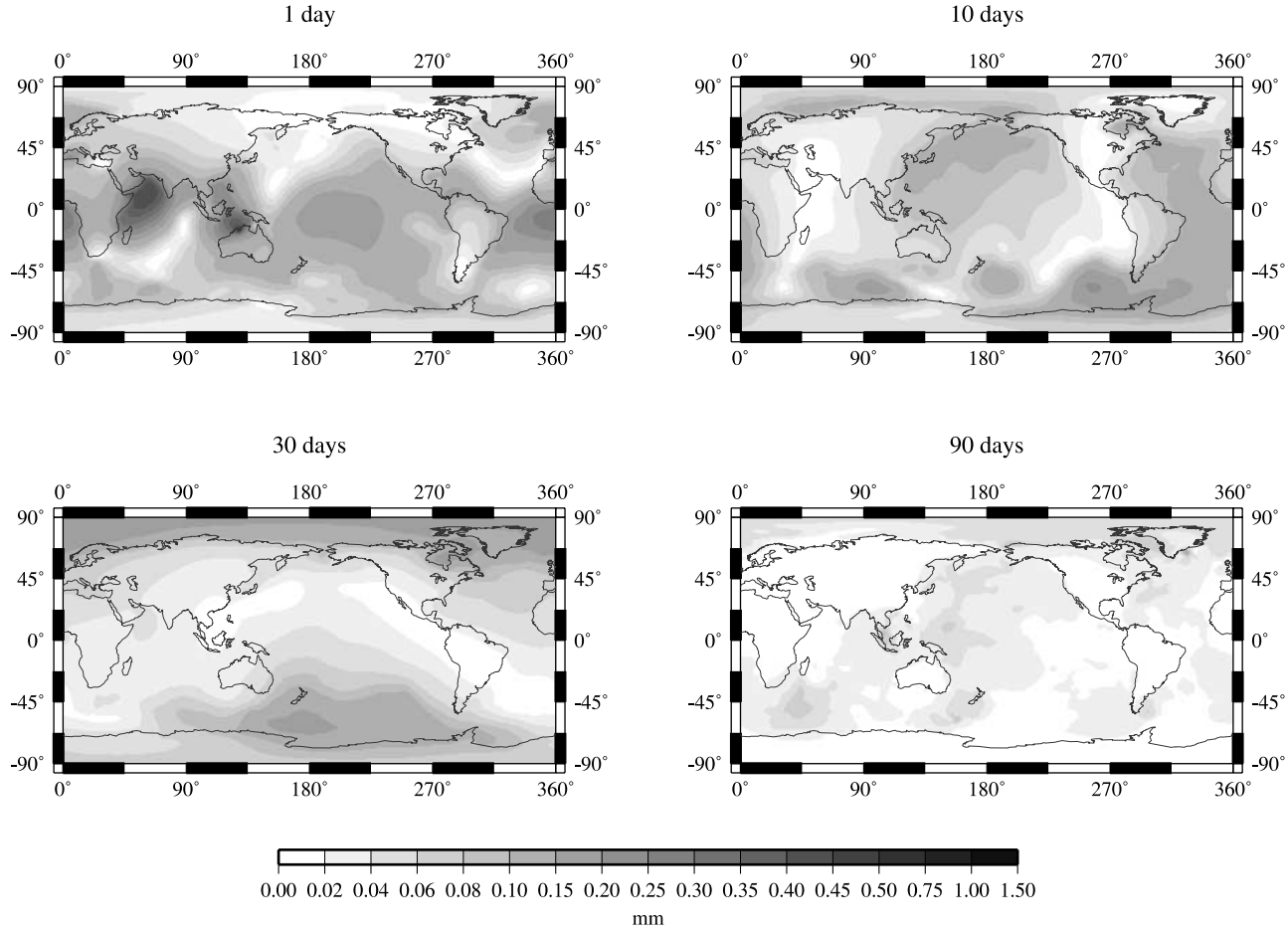

Figure 11. Shaded contour maps of geoid height variations induced by the departure from the IB assumption for the same periods as Figure 9.

However, potential aliasing problems due to mismodeling of the ocean response to pressure forcing in Indian Ocean may be significant.

[30] According to our computation, the response to the pressure forcing affects the gravitational fields up to degree 20 (2000 km or more) at high frequency. This effect is only above the precision limit for period shorter than 1 month.

6. Discussions and Conclusions

[31] In this paper, we compute some geodetic effects (polar motion, nutation, gravity change) of the ocean response to the atmospheric forcing, including the atmospheric pressure forcing.

[32] We show that the effect of the atmospheric pressure forcing is above the precision level for all the quantities we have investigated (polar motion, nutation, and gravity fields). Even if the model need to be improved to better represent the ocean response, mainly at very short periods, our results indicate that accounting for pressure forcing in the ocean dynamics is important for geodesy and can improve the modeling of geodetic observations.

[33] This is also true at period for which the IB approximation is usually considered as valid. *Ponte and Ali* [2002] have shown that their barotropic ocean model was able to very well model the high-frequency polar motion (<5 days). Nevertheless, their barotropic ocean model can only represent adequately the high frequencies, and miss part of the low-frequency dynamics of the ocean. The use of an adequately modified baroclinic ocean is important to allow using the same ocean model for the whole frequency band. Additionally, a barotropic ocean model cannot properly model the modulation of the high frequency ocean dynamics by the low-frequency baroclinic dynamics of the ocean.

[34] The results at diurnal frequency (and in particular for nutation) are given for information, as the comparison with in situ measurements showed that CLIO was overreacting as such high frequency. Additionally, we have to be careful with the nearly diurnal frequencies results, as they can only be as good as the atmospheric forcing is, at those frequencies. In particular, *Yseboodt et al.* [2002] have shown that the effect of atmosphere on nutation computed from different atmospheric models produce very different results. Consequently, as the pressure forcing dominates the atmospheric nutation excitation, it is difficult to assess to which extent the response of the ocean to GCM pressure forcing can be similar to the response of the true ocean to the real pressure forcing.

[35] An important part of the difficulties for the development and improvement of such a model is the absence of ''truths'' to compare with the OBP measurements are certainly to sparse to allow really a good comparison, which can be used in order to improve the model. The geodetic

quantities are always including a broad range of phenomena from the Earth deep interior (core effects) to the surface. Some of these effects, like hydrology, are still far from being known with a precision such that they can be used in geodesy. The additional constraints that will be given by geodetic satellite mission, like GRACE or ICESAT will certainly help to reach a global modeling of the Earth system, with better atmosphere, ocean, hydrology, ice coverage, which will, in return, allow a better modeling of the geodetic observations.

[36] **Acknowledgments.** The GLOUP data were found on http://www.pol.ac.uk/psmslh/gloup/gloup.html. The AAM data were found on the Web site of the IERS subbureau for the atmosphere (head, D. Salstein) at ftp://ftp.aer.com. The OAM data are from the Web site of the IERS subbureau for the ocean (head, R. Gross) at http://euler.jpl.nasa.gov/sbo. O.d.V. is a postdoctoral researcher of the Belgian National Fund for Scientific Research. H.G. is Research Associate at the Belgian National Fund for Scientific Research. T. Van Hoolst, R. Gross, J. Wahr, and an anonymous reviewer are acknowledged for their insightful comments on the manuscript.

References

Barnes, R. T. H., R. Hide, A. A. White, and C. A. Wilson (1983), Atmospheric angular momentum fluctuations, length-of-day changes and polar motion, *Proc. R. Soc. London, Ser. A*, *387*, 31–73.

Bizouard, C., A. Brzezinski, and S. Petrov (1998), Diurnal atmospheric forcing and temporal variations of the nutation amplitudes, *J. Geod.*, *72*, 561–577.

Campin, J.-M., and H. Goosse (1999), A parameterization of density-driven downsloping flow for a coarse-resolution model in *z*-coordinate, *Tellus, Ser. A*, *51*, 412–430.

Chao, B. F. (2003), Geodesy is not just for static measurements any more, *Eos Trans. AGU*, *84*, 145, 150.

Dehant, V., and O. de Viron (2002), Earth rotation as an interdisciplinary topic shared by astronomers, geodesists and geophysicists, *Adv. Space Res.*, *30*, 163–173.

Dehant, V., M. Feissel-Vernier, O. de Viron, C. Ma, M. Yseboodt, and C. Bizouard (2003), Remaining error sources in the nutation at the submilliarc second level, *J. Geophys. Res.*, *108*(B5), 2275, doi:10.1029/2002JB001763.

Deleersnijder, E., and J.-M. Campin (1995), On the computation of the barotropic mode of a free-surface world ocean model, *Ann. Geophys.*, *13*, 675–688.

de Viron, O., J. O. Dickey, and S. L. Marcus (2002), Effect of changes in total atmospheric mass on length-of-day modeling, *Geophys. Res. Lett.*, *29*(17), 1849, doi:10.1029/2002GL015572.

Dickey, J. O., et al. (1997), *Satellite Gravity and the Geosphere*, 112 pp., Natl. Acad. Press, Washington, D. C.

Dickey, J. O., S. L. Marcus, O. de Viron, and I. Fukumori (2002), Recent Earth oblateness variations: Unraveling climate and postglacial rebound effects, *Science*, *298*, 1975–1977.

Fichefet, T., and M. A. Morales Maqueda (1997), Sensitivity of a global sea ice model to the treatment of ice thermodynamics and dynamics, *J. Geophys. Res.*, *102*, 12,609–12,646.

Fichefet, T., B. Tartinville, and H. Goosse (2003), Antarctic sea ice variability during 1958–1999: A simulation with a global ice-ocean model, *J. Geophys. Res.*, *108*(C3), 3102, doi:10.1029/2001JC001148.

Fu, L.-L., and G. Pihos (1994), Determining the response of sea level to atmospheric pressure using TOPEX/POSEIDON data, *J. Geophys. Res.*, *99*, 24,633–24,642.

Gent, P. R., and J. C. McWilliams (1990), Isopycnal mixing in ocean circulation models, *J. Phys. Oceanogr.*, *20*, 150–155.

Goosse, H., E. Deleersnijder, T. Fichefet, and M. England (1999), Sensitivity of a global coupled ocean sea ice model to the parameterization of vertical mixing, *J. Geophys. Res.*, *104*, 13,681–13,695.

Goosse, H., J. M. Campin, E. Deleersnijder, T. Fichefet, P. P. Mathieu, M. A. Morales Maqueda, and B. Tartinville (2000), Description of the CLIO model Version 3.0, *Sci. Rep. 2000/3*, 49 pp., Inst. d'Astron. et de Geophys. G. Lematre, Louvain-la-Neuve, Belgium.

Gross, R. S. (2000), The excitation of the Chandler wobble, *Geophys. Res. Lett.*, *27*(15), 2329–2332.

Heiskanen, W., and H. Moritz (1967), *Physical Geodesy*, W. H. Freeman, New York.

Hibler, W. D., III (1979), A dynamic thermodynamic sea ice model, *J. Phys. Oceanogr.*, *9*, 815–846.

Hirose, N., I. Fukumori, V. Zlotnicki, and R. M. Ponte (2001), Modeling the high-frequency barotropic response of the ocean to atmospheric disturbances: Sensitivity to forcing, topography, and friction, *J. Geophys. Res.*, *106*(C12), 30,987–30,995.

Kalnay, E., et al. (1996), The NCEP/NCAR 40-year reanalysis project, *Bull. Am. Meteorol. Soc.*, *77*, 437–471.

Levitus, S. (1982), Climatological atlas of the world ocean, *NOAA Prof. Pap. 13*, 173 pp., U.S. Gov. Print. Off., Washington, D. C.

Marcus, S. L., Y. Chao, J. O. Dickey, and P. Gégout (1998), Detection and modeling of nontidal oceanic effects on the Earth's rotation rate, *Science*, *281*, 1656–1659.

Mathews, P. M., T. A. Herring, and B. A. Buffett (2002), Modeling of nutation and precession: New nutation series for nonrigid Earth and insights into the Earth's interior, *J. Geophys. Res.*, *107*(B4), 2068, doi:10.1029/2001JB000390.

Mellor, G. L., and T. Yamada (1982), Development of a turbulence closure model for geophysical fluid problems, *Rev. Geophys.*, *20*, 851–875.

Munk, W. H., and G. F. McDonald (1960), *The Rotation of the Earth, a Geophysical Discussion*, 323 pp., Cambridge Univ. Press, New York.

Ponte, R. M. (1993), Variability in a homogeneous global ocean forced by barometric pressure, *Dyn. Atmos. Oceans*, *18*, 209–234.

Ponte, R. M., and A. H. Ali (2002), Rapid ocean signals in polar motion and length of day, *Geophys. Res. Lett.*, *29*(15), 1711, doi:10.1029/2002GL015312.

Ponte, R. M., and P. Gaspar (1999), Regional analysis of the inverted barometer over the global ocean using TOPEX/POSEIDON data and model results, *J. Geophys. Res.*, *104*, 15,587–15,601.

Ponte, R. M., D. Stammer, and J. Marshall (1998), Oceanic signals in observed motions of the Earth's pole of rotation, *Nature*, *39*, 476–479.

Ray, R. D., D. D. Rowlands, and G. D. Egbert (2003), Tidal models in a new ara of satellite gravimetry, *Space Sci. Rev.*, *108*, 271–282.

Swenson, S., and J. Wahr (2002), Estimated effects of the vertical structure of atmospheric mass on the time-variable geoid, *J. Geophys. Res.*, *107*(B9), 2194, doi:10.1029/2000JB000024.

Tartinville, B., J.-M. Campin, T. Fichefet, and H. Goosse (2001), Realistic representation of the freshwater flux in an ice-ocean general circulation model, *Ocean Modell.*, *3*, 95–108.

Tierney, C., J. Wahr, F. Bryan, and V. Zlotnicki (2000), Short-period oceanic circulation: Implications for satellite altimetry, *Geophys. Res. Lett.*, *27*, 1255–1258.

Velicogna, I., J. Wahr, and H. Van de Dool (2001), Can surface pressure be used to remove atmospheric contributions from GRACE data with sufficient accuracy to recover hydrological signals?, *J. Geophys. Res.*, *106*, 16,415–16,434.

von Mises, R. (1964), *Mathematical Theory of Probability and Statistics*, 694 pp., Academic, San Diego, Calif.

Wahr, J., M. Molenaar, and F. Bryan (1998), Time-variability of the Earth's gravity field: Hydrological and oceanic effects and their possible detection using GRACE, *J. Geophys. Res.*, *103*, 30,205–30,230.

Wunsch, C., and D. Stammer (1997), Atmospheric loading and the "inverted barometer" effect, *Rev. Geophys.*, *35*, 117–135.

Yseboodt, M., O. de Viron, T. M. Chin, and V. Dehant (2002), Atmospheric excitation of the Earth's nutation: Comparison of different atmospheric models, *J. Geophys. Res.*, *107*(B2), 2036, doi:10.1029/2000JB000042.

O. de Viron, Royal Observatory of Belgium, Avenue Circulaire, 3, B-1180 Brussels, Belgium. (o.deviron@oma.be)

J.-P. Boy, EOST-IPG, Université Strasbourg, 5 rue René Descartes, F-67084 Strasbourg, France. (jpboy@eost.u-strasbg.fr)

H. Goosse, Institut d'Astronomie et de Géophysique Georges Lemaitre, Université catholique de Louvain, Chemin Cyclotron 2, B-1348 Louvain-La-Neuve, Belgium. (hgs@astr.ucl.ac.be)